Taylor & Francis
Taylor & Francis Group

Machining Science and Technology
An International Journal

ISSN: 1091-0344 (Print) 1532-2483 (Online) Journal homepage: https://www.tandfonline.com/loi/lmst20

Robust control synthesis for CNC machine spindle

Nguyen Ngoc Nam, Sam-Sang You, Boc Minh Hung, Pham Dinh Tung & Hwan-Seong Kim

To cite this article: Nguyen Ngoc Nam, Sam-Sang You, Boc Minh Hung, Pham Dinh Tung & Hwan-Seong Kim (2019): Robust control synthesis for CNC machine spindle, Machining Science and Technology

To link to this article: https://doi.org/10.1080/10910344.2019.1652310

Published online: 24 Sep 2019.

MACHINING SCIENCE AND TECHNOLOGY
https://doi.org/10.1080/10910344.2019.1652310

Robust control synthesis for CNC machine spindle

Nguyen Ngoc Nam[a], Sam-Sang You[a], Boc Minh Hung[a], Pham Dinh Tung[b], and Hwan-Seong Kim[c]

[a]Division of Mechanical Engineering, Korea Maritime and Ocean University, Busan, South Korea;
[b]Department of Aerospace Technology Engineering, Le Quy Don University, Hanoi, Vietnam;
[c]Division of Logistics Engineering, Korea Maritime and Ocean University, Busan, South Korea

ABSTRACT

This paper aims to analyze the dynamic stability and build the robust controller for motorized spindle system under parametric variations, external disturbances and measurement noises. A nonlinear model has been established for the machine tool spindles. The phase portrait and bifurcation analyses are provided to show dynamical behaviors for spindle machining. The spindle operations can be dynamically stables or unstable under parameter variations and disturbances. By using the robust control synthesis, the system designers can shape the frequency responses of the desired model which satisfies both transient response and robustness against various uncertainties. In fact, the robust controller can effectively attenuate exogenous disturbances and sensor noises during machining process. Finally, the simulations results demonstrate that the presented controller provides robust stability for the spindle speeds, along with excellent abilities of noise as well as disturbance attenuations.

KEYWORDS

Bifurcation; CNC spindle machine; machining process; robust controller; stability analysis

Introduction

A high speed machining system consists of several components such as machine tool, spindle and computer numerical control (CNC) system. Machine tools continue to make technical advances, thanks in large part to ongoing improvements in CNC machining. The CNC machine tools are complex dynamical systems applied to the machining process with speed and accuracy. One of the most essential functions in high-speed machining is the accurate guidance of the feed drives and spindles. In fact, the electric spindle control is the heart of the machining process. The disturbances and noises occurring during machine process should be reduced to achieve high accuracy and operational efficiency with desired surface roughness. The stable operations of the machine tools are essential to guarantee the high-quality of the finished products with low production costs. High-

CONTACT Sam-Sang You ssyou@Kmou.ac.kr Division of Mechanical Engineering, Korea Maritime and Ocean University, Busan 606-791, South Korea.

performance machining system can reduce high-risk of dynamic instability in the process. The loss of stability results in severe vibrations in the machining process. In turn, the machine tools can be damaged, and there will be difficulties in achieving high processing quality. Thus, machining stability plays a major role in enhancing improving tool performance and product quality. Nonlinear analysis of spindle speed system is essential to characterize the system dynamical behaviors. Based on this analysis, the robust controller is designed to keep the cutting process stable in CNC machine operations.

Many studies have been conducted to deal with nonlinear analysis and building the controller of spindle system to enhance the quality of precision products. Fuzzy control is utilized to synthesize the spindle system implementation (Liang et al., 2002; Liang et al., 2003; Haber-Guerra et al., 2006). The number of training iterations for finding the optimal parameters could be necessary for machining accuracy (Chiang et al., 1995; Lin and Wai, 2002; Karaye, 2009). More other approaches include intelligent adaptive control (Altintas, 1994; Liu et al., 1999), model adaptive control (Rober and Shin, 1996), self-tuning control (Hsu and Hsieh, 1994; Lian et al., 2006) and dynamic analysis of spindle system (Moon et al., 2006; Altintas et al., 2008). Due to the complexity of machining process, it is very difficult to properly identify the spindle parameters taking into account the cutting forces. Thus, the automatic controller is necessary to ensure high robustness and high-quality surface while coping with external disturbances in the machining process. Besides, the external disturbances and noises are not considered in the operations of existing most spindle control systems. Although there have been significant improvements in controlling machining processes, further progress still has to be made. Especially the effects on parameter variations and disturbances on the product quality are still to be studied to improve the system performance. This paper describes a systematic approach to analyze the nonlinear stability of spindle system considering the interaction of the machine tool, the work piece and cutting forces. In addition, the dynamic interactions of a rotating spindle-tool and a cutting work piece are considered by combining their respective transfer functions. The system dynamics are examined to identify the effects of the motor torques and the speed-dependent cutting forces. A constant diameter work piece is modeled to analyze the stability of the spindle tool structure. The numerical investigations are carried out to optimize the spindle speed, especially for industrial applications. The robust controller is designed for the spindle system to monitor the spindle speed under parameter uncertainties, measurement noises and external disturbances. In addition, the control synthesis aims to ensure the robust performance of the spindle system with low production costs and optimal energy usage. The paper is

organized as follows. Section 2 describes the mathematical system modeling with cutting forces interactions. Section 3 is dedicated to analyze equilibriums point and bifurcations of the spindle speed system. Section 4 presents the spindle controller by using robust control synthesis to guarantee optimal performance. Finally, the conclusions with discussions are given in Section 5.

Dynamical model of spindle system

For the high-speed machining process, the spindle system with the DC motor circuit is illustrated in Figure 1. Generally, the spindle system is rotated by adjusting the armature voltage of DC motor. The control synthesis considers not only the spindle dynamics, but also deals with the dynamic interactions between the spindle motions and the cutting forces. The nominal model of the spindle system can be described in (1). In addition, the rotational dynamics (Addasi, 2013) are described in (2–5).

$$T_m T_e \frac{d^2\omega}{dt^2} + T_m \frac{d\omega}{dt} + \omega = k_d U - k'_d U_m \tag{1}$$

$$U = R_a i_a + L_a \frac{di_a}{dt} + E \tag{2}$$

$$J_m \frac{d\omega}{dt} = M_e - M_t \tag{3}$$

$$M_e = C_m i_a \tag{4}$$

$$E = C_e \omega \tag{5}$$

where: U is the applied voltage (V); R_a is the armature resistance (Ω); i_a is armature current (A); L_a is the armature inductor (H); E is motor back electromotive force (V); ω is motor angular velocity (rad/s); M_e and M_t are the motor and load torque, respectively; and $J_m \frac{d\omega}{dt}$ is the torque acting on load inertia J_m (kg m^2).

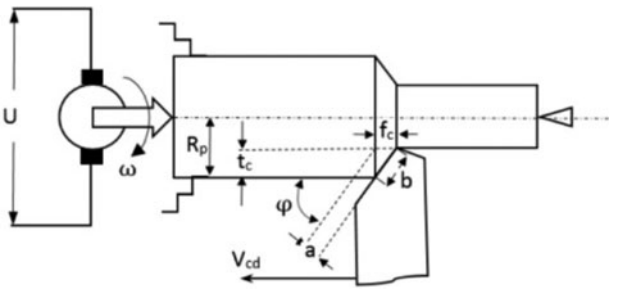

Figure 1. Schematic diagram of spindle drive system with cutting model.

By substituting (4) into (3), the current i_a can be further written as

$$i_a = \frac{J_m}{C_m}\frac{d\omega}{dt} + \frac{M_t}{C_m} \tag{6}$$

The applied voltage U can be determined by substituting (6) into (2) as follows;

$$\frac{L_a J_m}{C_m}\frac{d^2\omega}{dt^2} + \frac{L_a}{C_m}\frac{dM_t}{dt} + \frac{R_a J_m}{C_m}\frac{d\omega}{dt} + \frac{R_a}{C_m}M_t + C_e\omega = U \tag{7}$$

Then, it can be rewritten as

$$\frac{L_a R_a J_m}{R_a C_m C_e}\frac{d^2\omega}{dt^2} + \frac{R_a J_m}{C_m C_e}\frac{d\omega}{dt} + \omega = \frac{1}{C_m}U - \frac{1}{C_m}\frac{R_a}{C_m}\left(\frac{L_a}{R_a}\frac{dM_t}{dt} + M_t\right) \tag{8}$$

In addition, $T_e = \frac{L_a}{R_a}$ is armature time constant (s); $T_m = \frac{J_m R_a}{C_e C_m}$ is electrical time constant (s); $k_d = \frac{1}{C_m}$; $k'_d = \frac{R_a}{C_e C_m}$; C_m is the coefficient of ratio between motor torque and current; $U_m = \left(T_e\frac{dM_t}{dt} + M_t\right)$ is the voltage components caused by disturbance load torque; C_e is the coefficient of the ratio between dynamic force and the rotational speed of the motor.

To determine the influence of cutting force on the motor characteristics, the moment $M_{(t)}$ is considered in the voltage equation applied to motor, $U_m = \left(T_e\frac{dM_t}{dt} + M_t\right)$. This moment can be obtained by

$$M_{(t)} = R_P F = R_P.\lambda.\sigma.t_c \int_{t-T}^{t} V_{cd}dt \tag{9}$$

where R_p is the diameter of the work piece (mm); σ is the pressure of the chips on the tool face t_c is a depth of cut (mm); V_{cd} is cutting feed (mm/s); and λ is the coefficient.

Assuming that the tool velocity is constant, (9) can be given by

$$M_{(t)} = R_P F = R_P.\lambda.\sigma.t_c.T.V_{cd} = \frac{k_\omega}{\omega} \tag{10}$$

where $k_\omega = R_p.\lambda.\sigma.t_c V_{cd}$; $T = \frac{1}{\omega}$ is rotation period (s). Substituting (10) into (1), the complete dynamic model of the system which takes into account the cutting forces can be written by

$$T_m T_e\frac{d^2\omega}{dt^2} + T_m\frac{d\omega}{dt} + k_m\left(\frac{1}{\omega} - \frac{T_e d\omega}{\omega^2 dt}\right) + \omega = k_d U \tag{11}$$

where $k_m = k_\omega.k'_d$.

Nonlinear stability analysis

In order to characterize the dynamic behaviors, the spindle model can be described in the state-space representation. The stability characteristics are the dynamical performance with external disturbance, which accurately describes nonlinear system behaviors similar to bifurcation of the equilibrium points. Physically, for steady state handling analysis, the equilibrium points have more information than other points in any of the phase portraits. A small disturbance causes sensitive for unstable equilibrium points, and then any slight offset from the equilibrium point will lead to move away from the equilibrium solutions.

The system stability can be analyzed into two steps: firstly, phase portrait could be utilized by analyzing the system states around the equilibrium points. Secondly, the bifurcation analysis will be taken into account to evaluate the effect of multi-parameter variations on the stability of a real spindle system through the system eigenvalues.

Equilibriums and local dynamical analysis

To obtain a state-space model, the state variables are defined as follows: $x_1 = \omega$ and $x_2 = \dot{\omega}$ Then, the dynamical model described in (11) is given by

$$\begin{cases} \dot{x_1} = x_2 \\ \dot{x_2} = \dfrac{1}{T_e T_m}\left(\dfrac{k_m T_e}{x_1^2} - T_m\right)x_2 - \dfrac{k_m}{T_e T_m x_1} - \dfrac{1}{T_e T_m}x_1 + \dfrac{k_d U}{T_e T_m} \end{cases} \tag{12}$$

where x_1 is the spindle speed and x_2 is angular acceleration. The equilibrium points are found by setting the state derivatives to zero,

$$\begin{cases} x_2 = 0 \\ \dfrac{1}{T_e T_m}\left(\dfrac{k_m T_e}{x_1^2} - T_m\right)x_2 - \dfrac{k_m}{T_e T_m x_1} - \dfrac{1}{T_e T_m}x_1 + \dfrac{k_d U}{T_e T_m} = 0 \end{cases} \tag{13}$$

The equilibrium points can be obtained as follows: $EQ = \{Q_1(x_{11},0); Q_2(x_{12},0); \ldots; Q_n(x_{1n},0)\}$. To determine the system stability around equilibrium points, the spindle model can be linearized, using the Jacobian matrix J, as follows:

$$J = \begin{bmatrix} 0 & 1 \\ \dfrac{-1}{T_e T_m} + \dfrac{k_m}{T_e T_m x_1^2} - \dfrac{2k_m x_2}{T_m x_1^3} & \dfrac{k_m}{T_m x_1^2} - \dfrac{1}{T_e} \end{bmatrix} \tag{14}$$

The eigenvalues of Jacobian matrix are determined as follows:

$$\lambda_{1,2} = \frac{tr(J) \pm \sqrt{\left(tr(J)\right)^2 - 4\det(J)}}{2} \tag{15}$$

Table 1. The spindle model parameters.

Symbol	Values	Unit
R_a	1.48	Ω
L_a	0.01184	H
J	0.06	KJ m^2
U	220	V
I_a	22	A
k_m	15000	N
C_e	0.34	V s
C_m	1.08	N m A^{-1}

Based on the actual system equilibriums, the nonlinear dynamical analysis will be provided for the dynamic equations (12).

The spindle dynamic model is described with the nominal values of system parameters shown in Table 1. The rotational behaviors spindle can be depicted using the phase plane analysis. A phase portrait for the spindle system with cutting force $k = 15000(\mathrm{N})$ is shown in Figure 2a. The equilibrium points at $Q1$ and $Q2$ can be qualitatively specified as saddle and stable focus, respectively. The vector field analysis depicts that the state trajectories are converging to $Q1$, and the curves divide into the vector plane with many branches. All trajectories originating from the upper branches of the $Q1$ will tend to the point of stable focus $Q2$, while all trajectories originating from the lower branches of the $Q1$ will be away from $Q1$. Using the nominal parameter in Table 1, the system eigenvalues will be calculated as $\lambda_1 = -22.8663$ and $\lambda_2 = 96.2654$ at equilibrium point $Q1(55.554; 0)$, and $\lambda_{1,2} = -11.6027 \pm j17.8359$ at equilibrium point $Q2(270; 0)$.

The dynamical behaviors due to the increasing the cutting forces are shown in Figure 2b. Still, the equilibrium point $Q1(124; 0)$ is a saddle point, and the point $Q2(199; 0)$ is a stable focus. However, the range of the saddle point with the force ($k_m = 25000\,\mathrm{N}$) larger than that of the force ($k_m = 15000$ N). In turn, the range of the stable point is smaller than the previous one. In case of the cutting force ($k_m = 26146.89$ N), the spindle system has only one equilibrium point $Q(161.696; 0)$, with the eigenvalues of $\lambda_1 = 0.0054$ and $\lambda_2 = -6.73$, which is saddle point (161.7;0) as shown in Figure 2c. Physically, the dynamic features of the motor are changed by the cutting forces of the spindle system. The influence of cutting process on the spindle features depends on the motor parameters. If the cutting area is increased, the velocity of the spindle system shall decrease. The torque caused by cutting process shall be increased not proportionally but rapidly. When the load torque requires larger than the motor can provide the power, the machine will be stopped abruptly.

Bifurcation analysis

Base on the eigenvalue analysis, the stability of the system can be determined by two steady states: asymptotically stable equilibrium and

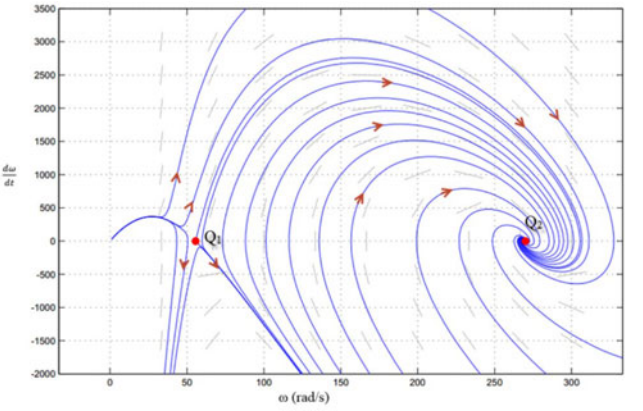

(a)

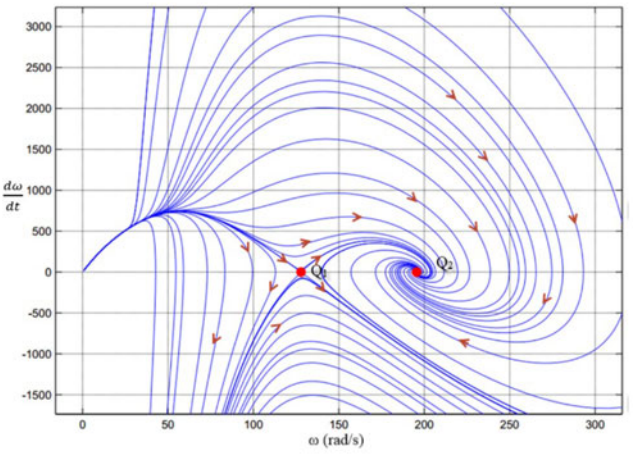

(b)

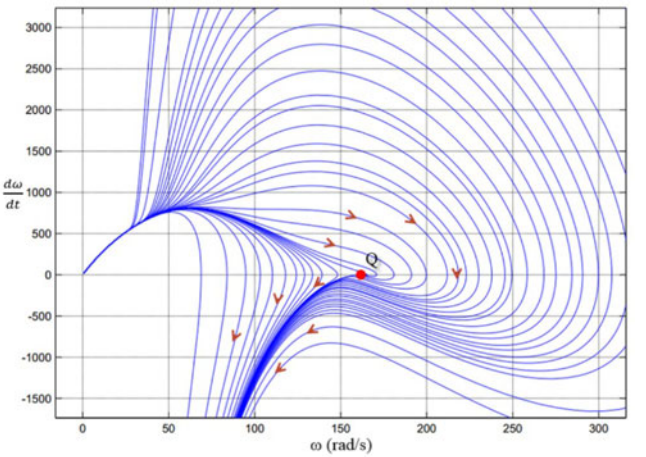

(c)

Figure 2. Phase portraits of the spindle behaviors with cutting forces: (a) $k_m = 15000$(N), (b) $k_m = 25000$ (N) and (c) $k_m = 26.146$ (kN).

a saddle point. The parameters of the spindle system are presented in Table 1. The basic parameters that affect the stability are; $R_p, \lambda, \sigma, T, V_{cd}$. Noting that, the coefficient λ depends on the temperature and the speed; σ depends on changes in the cutting layer size and variations in T corresponds to changes in cutting speed. In this case, parameters R_p and V_{cd} are considered as constants. All the parameters $(R_p, \lambda, \sigma, T, V_{cd})$ are interrelated to k_m both indirectly and directly and the changes to k_m will affect the individual parameters. Based on the parameters of the system shown in Table 1, the bifurcation diagram of the spindle system is illustrated in Figure 3a which is changing with the parameter supply voltage U. In Figure 3b the bifurcation diagram which is changing with the parameter cutting forces k_m is shown. Figure 3a shows the variations of the spindle speed with supply voltage at $k_m = 0$; the changes in spindle speed is stable over the supply voltage range. The rotational speed is directly proportional to supply voltage and hence the operation is more stable. In the case of $k_d U = 4k_m$, the spindle system has one equilibrium point and the system is unstable. In the other case, the spindle system has two equilibrium points corresponding two brand in the phase plane. Moreover, the stability of the over brand corresponds to the correlation $\left(k_d U + \sqrt{(k_d U)^2 + 4k_m}\right)/2$, represented by the solid line and instability of the under brand is represented by $\left(k_d U - \sqrt{(k_d U)^2 + 4k_m}\right)/2$, indicated using the dashed line. Figure 3b shows that, changing the cutting force parameter k_m, the spindle system behavior will change. In this case, the cutting force values ranges between; $0 < 4k_m < k_d U$, which results in the system having two equilibrium points. Of the two equilibrium points, one is stable and the other is unstable. The stable equilibrium point corresponds to $\left(k_d U + \sqrt{(k_d U)^2 + 4k_m}\right)/2$ indicated in a solid line in the over brand, and the unstable equilibrium points corresponds to $\left(k_d U - \sqrt{(k_d U)^2 + 4k_m}\right)/2$ shown in the dashed line in the under brand. In the others case, the system is unstable.

Both cases in Figures 3a, b, shows two cross-sections of the phase space. The straight lines $(A - A_1)$ divide the phase plane to two regions: X_1, the region of asymptotically stable equilibrium; X_2, the region of the saddle node. The equilibrium point becomes unstable when changing parameters such as supply voltage and cutting forces. Hence, depending on the supply voltage, cutting forces, the features of a product's surface can be enhanced. Thus, the best controller which can keep the stability of cutting forces must be considered.

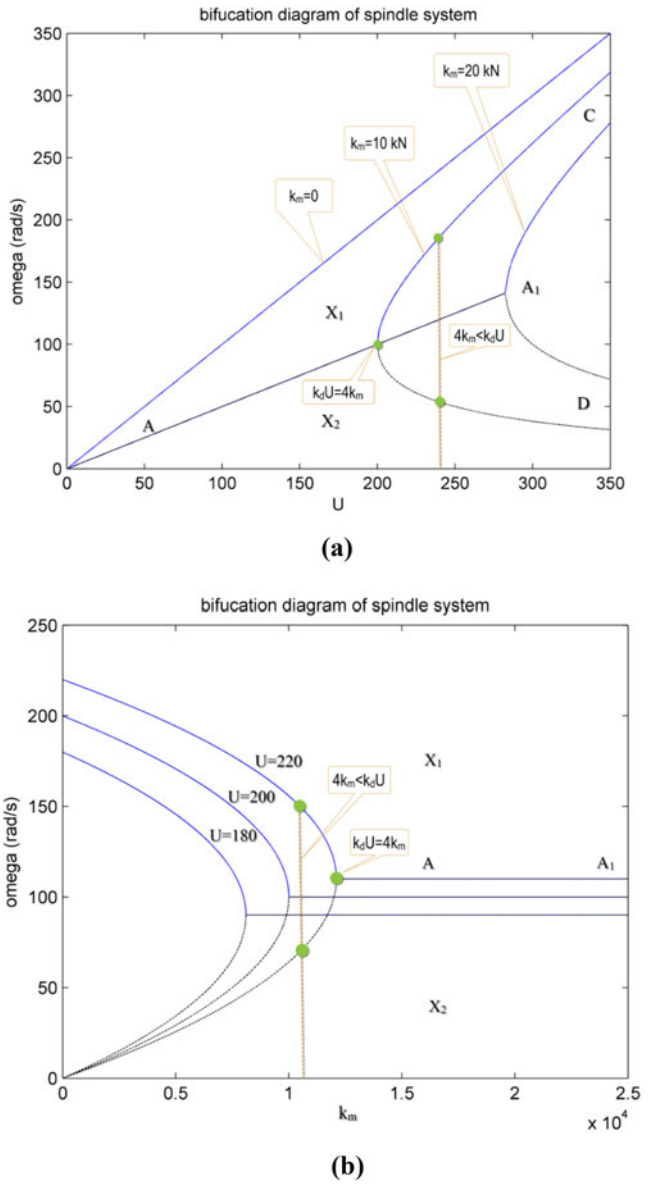

Figure 3. Bifurcation diagrams of the spindle system with parameters: (a) U and (b) k_m.

Robust control synthesis

Obtaining uncertainty model

Even if parametric uncertainty is difficult to be quantified, the frequency domain analysis is particularly well suited for uncertain dynamical model. When the complex perturbations are normalized such that $|\Delta|_\infty \leq 1$, the dynamic perturbation can be represented in form of multiplicative input uncertainty shown in Figure 4, and it can be described

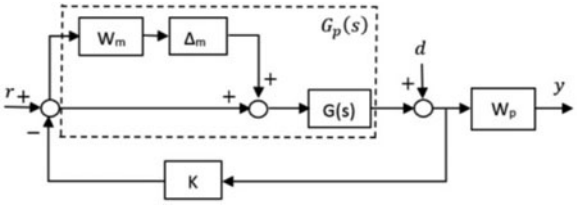

Figure 4. Uncertain dynamical model with multiplicative representation.

as following set ($\prod$):

$$\prod : G_P(s)\Big(1 + W_m(s)\Delta_m(s)\Big); \underbrace{\Big(|\Delta_m(j\omega)| \le 1\Big), \forall\omega}_{|\Delta_m|_\infty \le 1}$$

where $G(s)$ and $G_p(s)$ represent nominal and perturbed plants, respectively; $\Delta_m(s)$ is a stable transfer function which at each frequency is less than or equal to 1 of magnitude. A general procedure for handling parametric uncertainty (Skogestad and Postlethwaite, 2005) describes that a set of dynamic models can be represented as follows:

$$G_P(s) = \left[\begin{array}{c|c} A + \sum_{i=1}^{k} \alpha_i A_i & B + \sum_{i=1}^{k} \alpha_i B_i \\ \hline C + \sum_{i=1}^{k} \alpha_i C_i & D + \sum_{i=1}^{k} \alpha_i D_i \end{array}\right]$$

where the system matrices (A, B, C, D) represent the nominal model, and the parameter uncertainty is described by scalars $\alpha_i \in (-1, 1)$. The perturbed plant with uncertainty has a boundary of $l_m(j\omega)$ at each frequency. This boundary includes the possible plant $G_P(s) \in \prod$ defined by,

$$l_m(\omega) = \max_{G_p \in \Pi} \left| \frac{G_p(j\omega) - G(j\omega)}{G(j\omega)} \right| \tag{16}$$

Then the weighting function $W_m(s)$ is chosen to cover the boundary $l_m(j\omega)$ that satisfies as follows:

$$|W_m(j\omega)| \ge l_m, \ \forall\omega \tag{17}$$

Figure 5 illustrates the frequency responses for the boundary set of l_m and corresponding weighting function W_m. It can be seen that the weighting functions bound all the possible perturbed models, and the original plant $G_p(s)$ is covered by weighting function $W_m(j\omega)$.

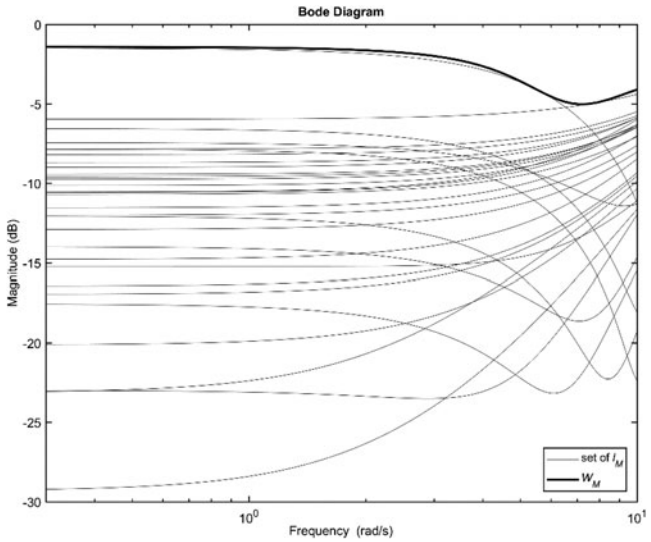

Figure 5. Bode plots of uncertainty weighting function.

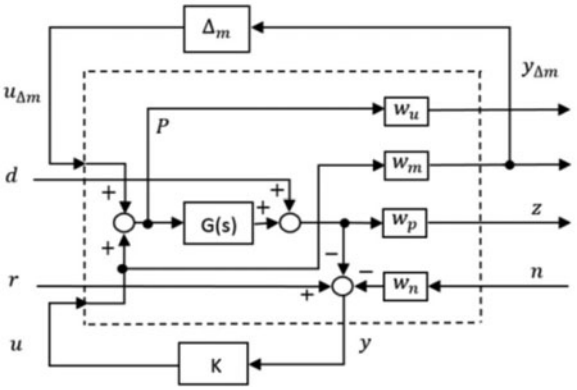

Figure 6. Complete control system with generalized plant P.

H_∞ control synthesis

The H_∞ control approach has been proved its ability to deal with the dynamical systems with disturbances and uncertainties. As shown in Figure 6, the plant $G(s)$ has been built to account all parameters affecting the spindle system dynamics. In this formulation, the system variables are described as follows: tracking error e, reference r, disturbance d, sensor noise n, measurement output y. The uncertainty at system input represented by w_m and Δ_m, which also accounts for unmolded high-frequency dynamics of spindle model. The weighting function w_p has added to the system output to guarantee the performance requirement. The controller K can be obtained by using $D-K$ iterations

that this dynamic compensator can deal with cutting force change, measurement noise and model uncertainty while satisfices robust performance and stability requirements.

The generalized plant P can be written as

$$\begin{bmatrix} y_{\Delta m} \\ z \\ \hline y \end{bmatrix} = P \begin{bmatrix} u_{\Delta m} \\ d \\ r \\ n \\ \hline u \end{bmatrix} \tag{18}$$

where

$$P = \left[\begin{array}{cccc|c} 0 & 0 & 0 & 0 & W_m \\ W_pG & W_p & 0 & 0 & W_pG \\ \hline -G & -I & I & -W_n & -G \end{array}\right] = \left[\begin{array}{c|c} P_{11} & P_{12} \\ \hline P_{21} & P_{22} \end{array}\right] \tag{19}$$

In order to utilize the robust control synthesis, the closed-loop transfer matrix N connects the generalized plant P with the controller K via a lower linear fractional transformation (LFT). Then the LFT will be calculated as

$$\begin{bmatrix} y_{\Delta m} \\ z \end{bmatrix} = N \begin{bmatrix} u_{\Delta m} \\ w \end{bmatrix}$$

where $w = [d \quad r \quad n]^T$ represent the exogenous input signals. This can be further written as

$$N = F_l(P,\ K) = P_{11} + P_{12}K(I - P_{22}K)^{-1}P_{21} \tag{20}$$

$$= \begin{bmatrix} -W_mT_i & -W_mKS_i & W_mKT_i & -W_mW_nKT_i \\ W_pG(I-T_i) & W_p(I-GS_i) & W_pGT_i & -W_pW_nGT_i \end{bmatrix} \tag{21}$$

where S_i and T_i are described as the sensitivity and complementary function, respectively.

According to the μ-synthesis framework, the optimal controller K are calculated as:

$$|N|_\infty = \max_\omega \bar{\sigma}\left(N(j\omega)\right) < 1 \tag{22}$$

where the maximum singular value $\bar{\sigma}(N(j\omega))$ is considered to measure the magnitude of transfer function matrix N at each frequency. Then the H_∞ optimal controller is obtained by

$$\min_K |F_l(P,\ K)|_\infty$$

where K is a stabilizing controller.

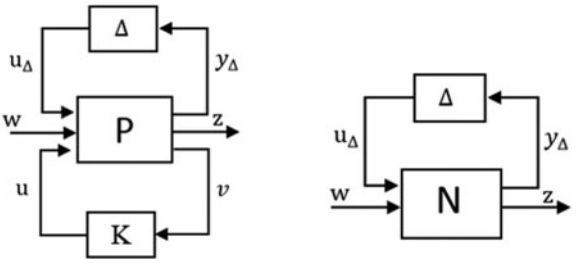

Figure 7. General configuration for control synthesis and $N\Delta$ - structure for control analysis.

Performance and stability analysis

Consider the uncertain system with $N\Delta$ - structure shown in Figure 7, where the block diagonal perturbations satisfy $|\Delta|_\infty \leq 1$. To analyze the performance and stability, the perturbed transfer function from external input w to output z can be evaluated by an upper LFT as follows:

$$M = F_u(N,\Delta) = N_{22} + N_{21}\Delta(I - N_{11}\Delta)^{-1}N_{12} \tag{23}$$

According to the μ-control synthesis with small gain theorem, $\mu_\Delta(N)$ represents the structured singular value of the system matrix N with respects to the uncertainty Δ. Then, the conditions for nominal performance (NP), robust stability (RS) and robust performance (RP) can be summarized as follows (Skogestad and Postlethwaite, 2005):

$$NS \Longleftrightarrow N(\text{internally})\ \text{stable} \tag{24}$$

$$NP \Longleftrightarrow \bar{\sigma}(N_{22}) = \mu_{\Delta_p}(N_{22}) < 1,\ \forall\omega \text{ and } NS \tag{25}$$

$$RS \Longleftrightarrow \mu_\Delta(N_{11}) < 1,\ \forall\omega \text{ and } NS \tag{26}$$

$$RP \Longleftrightarrow \mu_\Delta(N) < 1,\ \forall\omega;\ \Delta = \begin{bmatrix} \Delta & 0 \\ 0 & \Delta_p \end{bmatrix}, \text{ and } NS \tag{27}$$

where Δ is a block-diagonal matrix, and Δ_p is a full complex matrix representing H_∞ performance specification.

Figure 8 illustrates the structured singular value curves for the closed-loop systems with controller K. It is shown that $NP = 0.143$, $RS = 0.139$ and $RP = 0.139$. Thus all stability and performance tests have been passed by checking the requirements specified above. Figure 9 shows that the worst case performance degradation of the weighted sensitivity function is described as the size of uncertainty. Based on the performance analysis, the controller K will stabilize the perturbed plant with ensuring robust performance.

Test results and discussions

The robust controller is designed to cope with parameter uncertainties, noises and disturbances. It is noted that the cutting force k_m is severely

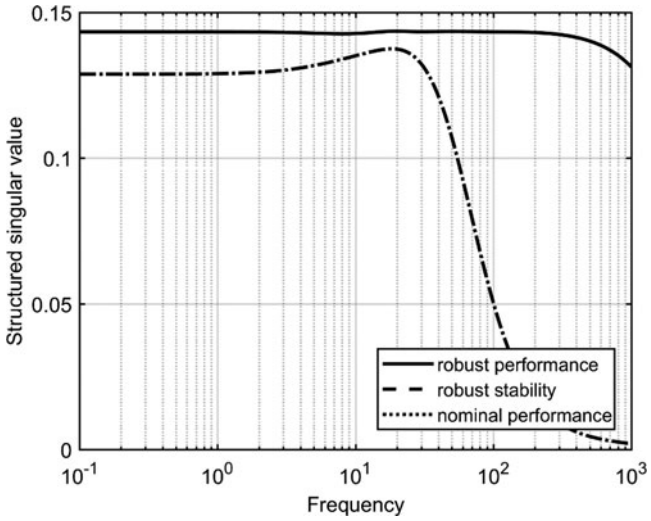

Figure 8. Structured singular value plot with robust controller.

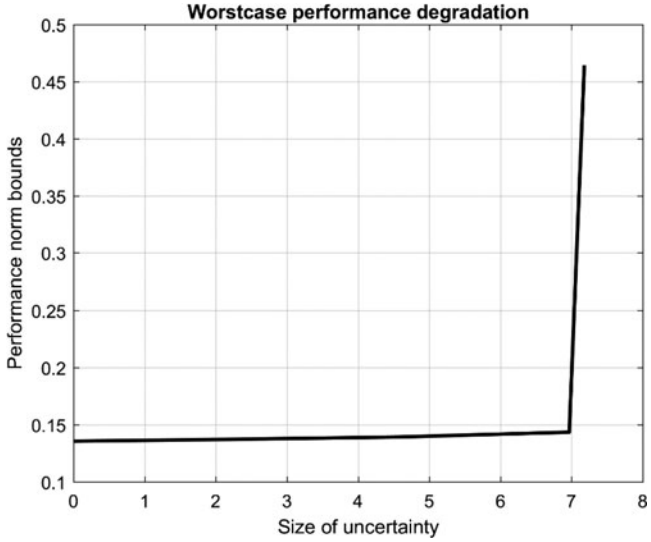

Figure 9. Performance degradation against magnitude of uncertainty.

changing during machining. Thus, the influence cutting force will be attenuated on motor spindle system by using robust controller. In fact, all spindle parameters shown in Table 1 are subjected to parameter variations during machining. For the robust control synthesis, a set of suitable weighting functions should be selected to guarantee the design specifications given by (22). From the system responses illustrated in Figure 10, it can be observed that there are small performance differences between the three spindle models: minimum model, nominal model and maximum model. All the responses are fast enough with rising times less than 2 s, and there exists no overshoot with the nominal model and minimum model.

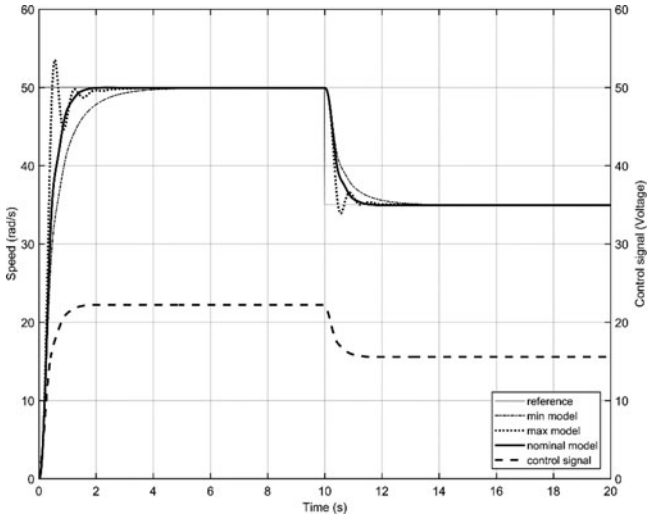

Figure 10. Transient responses for the spindle speed with robust controller.

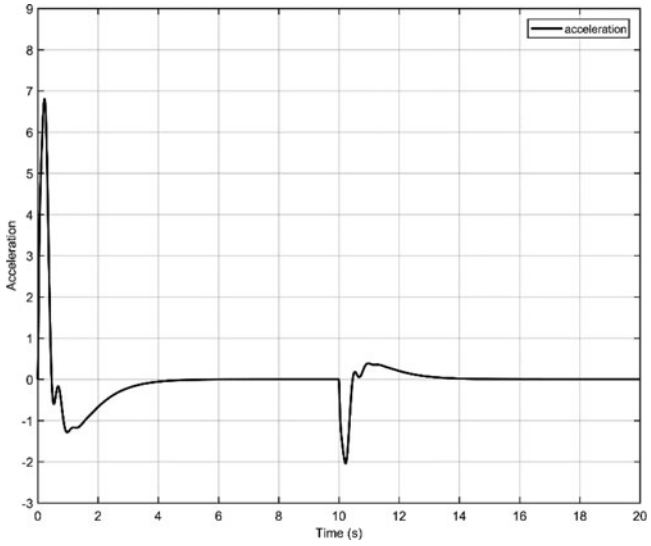

Figure 11. Transient responses for the spindle acceleration with robust controller.

Even the overshoot of the maximum model is approximately 7%. Also, the control activity shows that increasing the control signal will increase the velocity and decreasing the control signal will reduce the velocity.

The angular acceleration of spindle system is shown in Figure 11, where the spindle speed has direct effects on acceleration.

In the actual machining process, the measured outputs are always contaminated by sensor noises. The distorted signals by noises often occur in high-frequency ranges. The controller should effectively eliminate the distorted noises to ensure robust system performance. As illustrated in Figure 12, it can be observed that 93% of noises in the spindle system

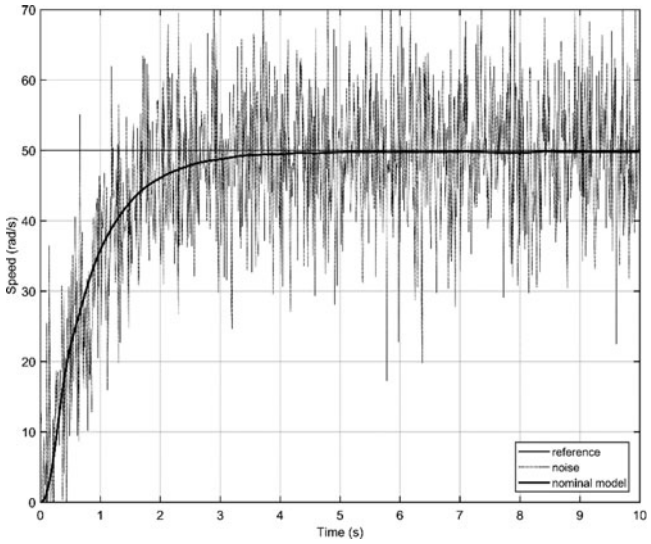

Figure 12. Time-domain system responses due to sensor noises with robust controller.

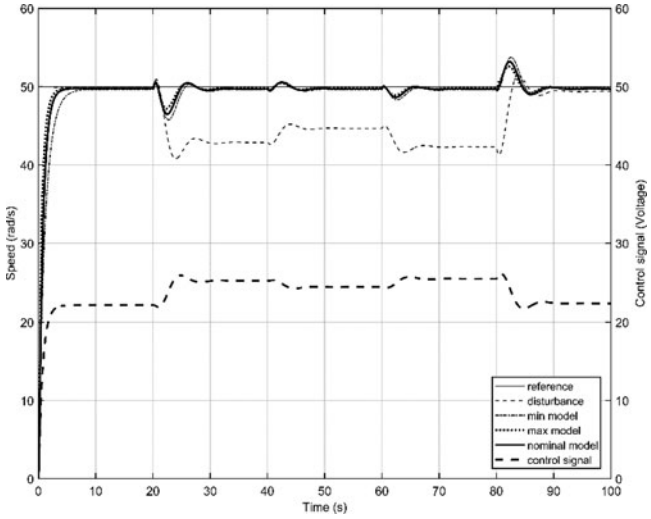

Figure 13. Time-domain system responses due to disturbances with robust controller.

successfully removed. This means that the robust controller can provide safe machining operations for the spindle system under large distortions caused by noises.

In addition, the major emphasis is on the ability of the disturbance attenuation of the robust control system, while the ability to follow reference signals is the primary concern. Figure 13 shows that the cutting forces with tool vibrations and temperature effects are all lumped into exogenous disturbance vector d to the spindle system. The cutting process causes tool vibrations and machine chattering that degrade part surface quality and eventually damage machine tools. One of approaches is to design the powerful

controller to handle external disturbances. In addition to the reference inputs, the assumed disturbances have been applied to real machining processes. Specifically, the disturbance in angular velocity from 50 rad/s by a magnitude of 10 rad/s to 40 rad/s occurred over a response time of 7 s. Also, increasing the disturbance will automatically increase the signal control and vice versa. Constant disturbance results in constant signal control. This consequently results in a robust and powerful controller that can minimize disturbance and maintain stable operation for the spindle system. Figure 13 depicts that at least 95% of disturbance is effectively eliminated in transient state and the disturbance is completely removed in steady-state. It is also worth noting that the motion fluctuations occur in a very short time. Hence, the spindle system is under control and stable even against large disturbance.

Given the nominal values of the model parameters in Table 1, the controlled system can effectively cope with those parameter changes by decreasing influence of the cutting force on the properties of the spindle system, resulting in good quality operation and excellent performance capabilities.

Conclusions

This paper deals with the dynamical analysis and robust control synthesis for spindle machining system. For the given nonlinear model, the vector field diagrams have been provided for qualitative information of the spindle speed dynamics. The stability analysis with bifurcation diagram is given for exploring dynamical behaviors of the spindle system. The linearization model around equilibrium points has been obtained for synthesizing robust controller. In general, designing spindle control system is very a challenging problem due to its parameter uncertainty and exogenous inputs (disturbances and sensor noises). The robust controller has been successfully designed to cope with these difficulties for guaranteeing optimal spindle operations. By using multiplicative uncertainty description, the parametric uncertainty can be modeled in the general form, which captures both high frequency unmolded dynamics and physical parameter variations. The time-domain responses are provided by measuring rise time, peak time, maximum overshoot and settling time, especially, with the rise time of less than 2 s. The comprehensive test results show that the robust controller can attenuate approximately 100% of external disturbances and sensor noises in the steady-state, guaranteeing robust machining operations. Based the complete analyses on dynamic behaviors, model optimization and the robust control synthesis, this work provides remarkable contributions on plant monitoring. Finally, the presented control approaches are considered as essential to safe and reliable process operations of machine tools.

Funding

This research was supported by a grant (17LRP-B079281-04) from Transportation & Logistics Research Program funded by Ministry of Land, Infrastructure and Transport of Korean government.

References

Addasi, E.S. (2013) Modelling and simulation of DC motor electric drive control system with variable moment of inertia. *ACEEE International Journal on Electrical and Power Engineering*, *4*(1): 52–57.

Altintas, Y. (1994) Direct adaptive control of end milling process. *International Journal of Machine Tool & Manufacture*, *34*(4): 461–472.

Altintas, Y.; Eynian, M.; Onozuka, H. (2008) Identification of dynamic cutting force coefficients and chatter stability with process damping. *CIRP Annals* Manufacture *Technology*, *57*(1): 371–374.

Chiang, S.T.; Liu, D.I.; Lee, A.C.; Chieng, W.H. (1995) Adaptive control optimization in end milling using neural network. *International Journal of Machine Tools and Manufacture*, *35*(4): 637–660.

Haber-Guerra, R.; Liang, S.Y.; Alique, J.R.; Haber-Haber, R. (2006) Fuzzy control of spindle torque in high-speed milling processes. *Journal of Manufacturing Science & Engineering*, *128*(4): 961–969.

Hsu, P.L.; Hsieh, M.Y. (1994) Applications of self-turning control on industrial CNC machines. *International Journal of Machine Tool & Manufacture*, *34*(6): 859–877.

Karaye, D. (2009) Prediction and control of surface roughness in CNC lathe using artificial neural network. *Journal of Materials Processing Technology*, *209*(7): 3125–3137.

Lian, R.J.; Lin, B.F.; Huang, J.H. (2006) Self-organizing fuzzy control of constant cutting force in turning. *The International Journal of Advanced Manufacturing Technology*, *29*(5): 436–445.

Liang, M.; Yeap, T.; Hermansyah, A.; Rahmati, S. (2003) Fuzzy control of spindle torque for industrial CNC machining. *International Journal of Machine Tools and Manufacture*, *43*(14): 1497–1508.

Liang, M.; Yeap, T.; Rahmati, S.; Han, Z. (2002) Fuzzy control of spindle power in milling processes. *International Journal of Machine Tools and Manufacture*, *42*(14): 1487–1496.

Lin, F.J.; Wai, R.J. (2002) Adaptive fuzzy neural network control for induction spindle motor drive. *IEEE Transaction on Energy Conversion*, *17*(4): 507–513.

Liu, Y.; Zuo, L.; Wang, C. (1999) Intelligent adaptive control in milling processes. *International Journal of Computer Integrated Manufacturing*, *12*(5): 453–460.

Moon, J.D.; Kim, B.S.; Lee, S.H. (2006) Development of the active balancing for high speed spindle system using influence coefficients. *International Journal of Machine Tools and Manufacture*, *46*(9): 978–987.

Rober, S.J.; Shin, Y.C. (1996) Control of cutting force for end milling processes using an extended model reference adaptive control scheme. *Journal of Manufacturing Science and Engineering*, *118*(3): 339–347.

Skogestad, S.; Postlethwaite, I. (2005) *Multivariable feedback control analysis and design*, 2nd edn. John Wiley & Sons Ltd, England.